

A LOW-RANK NON-CONVEX NORM METHOD FOR MULTIVIEW GRAPH CLUSTERING

A. ZAHIR*, K. JBILOU*[†], AND A. RATNANI*

Abstract. This study introduces a novel technique for multi-view clustering known as the "Consensus Graph-Based Multi-View Clustering Method Using Low-Rank Non-Convex Norm" (CGMVC-NC). Multi-view clustering is a challenging task in machine learning as it requires the integration of information from multiple data sources or views to cluster data points accurately. The suggested approach makes use of the structural characteristics of multi-view data tensors, introducing a non-convex tensor norm to identify correlations between these views. In contrast to conventional methods, this approach demonstrates superior clustering accuracy across several benchmark datasets. Despite the non-convex nature of the tensor norm used, the proposed method remains amenable to efficient optimization using existing algorithms. The approach provides a valuable tool for multi-view data analysis and has the potential to enhance our understanding of complex systems in various fields. Further research can explore the application of this method to other types of data and extend it to other machine-learning tasks.

1. Introduction. Multiview data clustering is a difficult machine learning task that requires combining data from several data sources or perspectives to cluster data points precisely. In many disciplines, including computer vision, neurobiology, and social network research, multi-view data are frequently encountered. The underlying relationships between viewpoints may not be captured well by conventional clustering approaches that examine each view independently, yielding less-than-ideal clustering outcomes. Thus, it's crucial to create processes that can efficiently utilize information from various points of view.

Another method that has been extensively utilized for multi-view data analysis is tensor decomposition [1]. The underlying relationships between views can be captured via latent components that can be extracted using tensor decomposition to represent multi-view data as high-order tensors. Popular tensor decomposition techniques, such as non-negative matrices and tensor factorization (NMF and NTF), have been used in multi-view clustering [2].

In this paper, we propose a new method for multi-view clustering that uses a non-convex tensor norm. The proposed method (CGMVC-NC) utilizes the tensor structure of multi-view data and introduces a non-convex tensor norm to capture the correlations between views. The non-convexity of the tensor norm allows it to model complex and non-linear relationships between views. Compared to traditional methods, the proposed method achieves better clustering accuracy on several benchmark datasets.

The contributions of this paper are summarized as follows:

- 1 We propose a novel multi-view clustering method that performs spectral embedding and tensor representation with a parametric non-convex tensor norm.
- 2 We propose an alternating optimization algorithm to solve the proposed problem. The experimental results validated our approach.

The remainder of this paper is organized as follows. In section 2, we will give some preliminaries to include the tensor related theories as norm and multiplication. In Section 3, we review related work on multi-view clustering and tensor decomposition. In Section 4, we present the proposed method for multi-view clustering using a non-convex tensor norm. In Section 5, we evaluate the proposed method on several benchmark datasets and compare it to state of art methods. Finally, in the final section, we conclude the paper and discuss future research directions.

*The UM6P Vanguard Center, Mohammed VI Polytechnic University, Green City, Morocco.

[†]Université du Littoral Cote d'Opale, LMPA, 50 rue F. Buisson, 62228 Calais-Cedex, France.

2. Preliminaries. This section presents some preliminaries and notations related to this subject. We focus on third-order tensors $\mathcal{X} \in \mathbb{R}^{N_1 \times N_2 \times N_3}$. We define the frontal slices of \mathcal{X} , denoted by $X^{(1)}, \dots, X^{(N_3)}$, referred to fixing the last index.

We define $\tilde{\mathcal{X}}$ as the discrete Fast Fourier transform (FFT) of \mathcal{X} along the third dimension, that is, in MATLAB syntax, $\tilde{\mathcal{X}} = \text{fft}(\mathcal{X}, [], 3)$.

The transpose of \mathcal{X} denoted by $\mathcal{X}^T \in \mathbb{R}^{N_2 \times N_1 \times N_3}$ is obtained by transposing each frontal slice and then reversing the order of transposed frontal slices 2 through N_3 .

A tensor is called, orthogonal if it satisfies the relationship:

$$\mathcal{X}^T * \mathcal{X} = \mathcal{X} * \mathcal{X}^T = \mathcal{I}.$$

Where $*$ referred here [3] to the T-product. A tensor is called, f-diagonal if each of its frontal slices is a diagonal matrix. The T-SVD decomposition theorem [3, 4, 5] states that \mathcal{X} can be factorized as:

$$\mathcal{X} = \mathcal{U} * \mathcal{S} * \mathcal{V}^*, \quad (2.1)$$

where $\mathcal{U} \in \mathbb{R}^{N_1 \times N_1 \times N_3}$, $\mathcal{V} \in \mathbb{R}^{N_2 \times N_2 \times N_3}$ are orthogonal and $\mathcal{S} \in \mathbb{R}^{N_1 \times N_2 \times N_3}$ is f-diagonal tensor. Next, we define some norms, starting with the Frobenius norm and the nuclear norm[6]:

$$\begin{aligned} \|\mathcal{X}\|_F^2 &= \sum_{i,j,k} \mathcal{X}_{ijk}^2. \\ \|\mathcal{X}\|_{\otimes} &= \sum_{i=1}^{N_3} \|\tilde{X}^{(i)}\|_*, \end{aligned} \quad (2.2)$$

where $\|\cdot\|_*$ is the nuclear norm of matrix, which is exactly the sum of the singular values. It is proven [6] to be a valid norm and the tightest convex relaxation to the norm of the tensor average rank within the unit ball of the tensor spectral norm.

We can further define a generalization of this norm called the weighted tensor nuclear norm :

$$\|\mathcal{X}\|_{\omega, \otimes} = \sum_{i=1}^{N_3} \|\tilde{X}^{(i)}\|_{\omega, *} = \sum_{i=1}^{N_3} \sum_{j=1}^{\min(N_1, N_2)} \omega_j \sigma_j(\tilde{X}^{(i)}),$$

where $\sigma_j(Z)$ denotes the j -largest singular value of the matrix Z .

Another norm that will be presented is the t-Gamma tensor quasi-norms presented in [7], defined as:

$$\|\mathcal{X}\|_{t-\gamma} = \frac{1}{N_3} \sum_{n_3=1}^{N_3} \|\tilde{X}^{(n_3)}\|_{\gamma},$$

where, $\|\cdot\|_{\gamma}$ represents the Gamma quasi-norm for matrices [8], for $Z \in \mathbb{R}^{N_1 \times N_2}$

$$\|Z\|_{\gamma} = \sum_{i=1}^{\min(N_1, N_2)} \frac{(1 + \gamma)\sigma_i(Z)}{\gamma + \sigma_i(Z)}, \gamma > 0.$$

3. Related work. The multi-view clustering [9] approaches can be roughly divided into two types based on how the similarity graph is constructed: subspace segmentation-based methods and graph-based methods.

Multi-view subspace clustering attempts to discover a latent space from all the different views to deal with high-dimensional data and then applies a traditional clustering approach to this subspace.

Two exemplary of single view clustering techniques are low rank subspace clustering (LRR) [10] and sparse subspace clustering (SSC) [11]. Several multi-view subspace clustering techniques [12, 13] have been proposed based on LRR and SSC. i.e, according to the experimental results in [14], the LRR miscategorizes different data points than SSC. Thus, low-rank and sparsity criteria must be coupled to capture both the global and local structure of the data [14]. In [14], the authors proposed a multi-view subspace clustering method based on the coupled low-rank and sparse representation (CLRS) model.

Treating data as matrices rather than as a full tensor implies that the relationship between subspaces is overlooked; thus, various approaches [15, 16, 17] transform data into a third-order tensor to capture high-order view correlations.

Multi-view graph clustering aims to find a fusion graph of all views, then applies the classical clustering methods on the fusion graph, as spectral clustering or graph-cut algorithms to produces the final clustering. In [18], canonical correlation analysis (CCA) is used to identify the common underlying structure between different views. Although it does not give importance to the weight, in [19], it adds new hyper parameters. In AMGL method [20], there are no hyper parameters, it can learn the weight by itself. In [21, 22], these methods are based on the generalization of the Laplacian rank constrained to give a similarity matrix with exactly the desired number of components. As in the subspace based method [23, 24, 25, 26], data is transformed into a tensor to capture the high-order view correlations within the data.

Noise and redundant information are typically mixed with the original characteristics in practice. Consequently, the learned consensus similarity graph may be incorrect. To overcome this problem, [26], proposed an approach called Consensus graph learning (CGL), which trains an adaptive neighbor graph in a new low-dimensional embedding space rather than the original feature space. First, it learns the view-specific similarity graph $S^{(v)}$ using adaptive neighbor graph learning:

$$\begin{aligned} \forall i = 1, \dots, n \quad \min_{S_i^{(v)}} \sum_{j=1}^n \left\| \mathbf{x}_i^{(v)} - \mathbf{x}_j^{(v)} \right\|_2^2 S_{ij}^{(v)} + \gamma s_{ij} \\ s_{ij}^{(v)} \geq 0, \mathbf{1}^T \mathbf{s}_i^{(v)} = 1, j = 1, \dots, n, \end{aligned} \quad (3.1)$$

the new low-embedding space is learned as follows:

$$\begin{aligned} \min_{F^{(v)}, \mathcal{T}} -\lambda \sum_{v=1}^V \text{tr} \left(F^{(v)} A^{(v)} F^{(v)T} \right) + \frac{1}{2} \|\mathcal{F} - \mathcal{T}\|_F^2 + \|\mathcal{T}\|_{w,*} \\ \text{s.t. } F^{(v)T} F^{(v)} = I_c, v = 1, \dots, V \\ \mathcal{F} = [\overline{F}^{(1)} \overline{F}^{(1)T}; \dots; \overline{F}^{(n)} \overline{F}^{(n)T}], \end{aligned} \quad (3.2)$$

where the normalized spectral embedding matrix $\overline{F}^{(v)}$ is obtained by normalizing the rows of $F^{(v)}$, the normalized affinity matrix is given

$$A^{(v)} = D^{(v)-0.5} S^{(v)} D^{(v)0.5}, \quad (3.3)$$

where $D^{(v)}$ is a diagonal matrix containing the sum of elements of the affinity matrix and the tensors $\mathcal{F}, \mathcal{T} \in \mathbb{R}^{n \times V \times n}$, to which the consensus graph S can be learned in the last step using

the adaptive neighbour again as:

$$\min_S \sum_{v=1}^V \left(\sum_{i,j=1}^n \left\| \bar{\mathbf{f}}_i^{(v)} - \bar{\mathbf{f}}_j^{(v)} \right\|_2^2 s_{ij} + \frac{\gamma}{V} s_{ij} \right) \quad (3.4)$$

$$s_{ij} \geq 0, \mathbf{1}^T \mathbf{s}_i = 1, i, j = 1, \dots, n.$$

4. Proposed method.

4.1. Data. Given multi-view data $\{X^{(v)}\}_{v=1,\dots,V}$ where $X^{(v)} = [\mathbf{x}_1^{(v)}, \dots, \mathbf{x}_n^{(v)}] \in \mathbb{R}^{d_v \times n}$ is the data matrix of the v -th view, d_v is the dimension of features in view v , n is the number of data points and V is the number of views. The goal of multi-view clustering is to learn a consensus clustering result from multiple views. In this paper, we assume that the data points are from k clusters, and the clustering result $Y \in \mathbb{R}^n$ is a discrete vector with $Y_i \in \{1, \dots, k\}$, $i = 1, \dots, n$. The clustering result Y is unknown and needs to be learned from the multi-view data.

4.2. Graph construction. The graph construction is the first step in the method, the most common method are the k-nearest neighbor (kNN), the ϵ -neighborhood graph and the complete graph. The kNN graph is constructed by connecting each data point to its k-nearest neighbors. The ϵ -neighborhood graph is constructed by connecting each data point to its neighbors within a radius ϵ . The complete graph put an edge between all points. The result is an affinity matrix, where the weight of the edge, is commonly computed using:

- Gaussian kernel: $s_{ij}^{(v)} = \exp\left(-\frac{\|\mathbf{x}_i^{(v)} - \mathbf{x}_j^{(v)}\|_2^2}{2\gamma}\right)$, where γ is a scaling parameter.
- Cosine similarity: $s_{ij}^{(v)} = \frac{\mathbf{x}_i^{(v)T} \mathbf{x}_j^{(v)}}{\|\mathbf{x}_i^{(v)}\|_2 \|\mathbf{x}_j^{(v)}\|_2}$
- Euclidean distance: $s_{ij}^{(v)} = \frac{1}{\|\mathbf{x}_i^{(v)} - \mathbf{x}_j^{(v)}\|_2}$
- Binary: $s_{ij}^{(v)} = 1$.

In this paper, we will stick with the adaptive neighbour graph, which is a combination of the kNN and the ϵ -neighborhood graph. The adaptive neighbor graph is constructed by connecting each data point to its k-nearest neighbors, and then, for each data point, the weight of the edge is computed as the distance between the data point and its k+1 nearest neighbor. The weight of the edge is computed using the Euclidean distance.

4.3. Problem formulation. Since in equation (3.2), Since we've previously attained the tightest convex low-rank as a norm, we suggest loosening the convexity restriction using the Non-Convex Low Rank to improve the probability of reaching the norm, i.e. the t-Gamma tensor quasi-norm. The Gamma tensor quasi-norm has some algebraic properties. It is positive definite and unitarily invariant, its limits are exactly the tubal rank when $\gamma \rightarrow 0$, and the tensor nuclear norm when $\gamma \rightarrow +\infty$. It has shown some promising results in terms of accuracy and efficiency [8]. It can overcome the imbalanced penalization by different singular values in the convex nuclear norm. Therefore, we propose a new approach called Consensus graph-based multi view clustering using a low-rank non convex norm (CGMVC-NC). We suggest to change

problem (3.2) to become:

$$\begin{aligned}
 \min_{F^{(v)}, \mathcal{T}} & \left[-\lambda \sum_{v=1}^V \text{tr} \left(F^{(v)} A^{(v)} F^{(v)T} \right) + \frac{1}{2} \|\mathcal{F} - \mathcal{T}\|_F^2 + \rho \|\mathcal{T}\|_{t-\gamma} \right] \\
 \text{s.t. } & F^{(v)} \in V_c(\mathbb{R}^n), v = 1, \dots, V \\
 & \mathcal{F} = [\bar{F}^{(1)} \bar{F}^{(1)T}; \dots; \bar{F}^{(V)} \bar{F}^{(V)T}].
 \end{aligned} \tag{4.1}$$

where the Stiefel manifold $V_c(\mathbb{R}^n)$ is the set of all $n \times c$ matrices with orthonormal columns. We can provide the framework of the problem as follows:

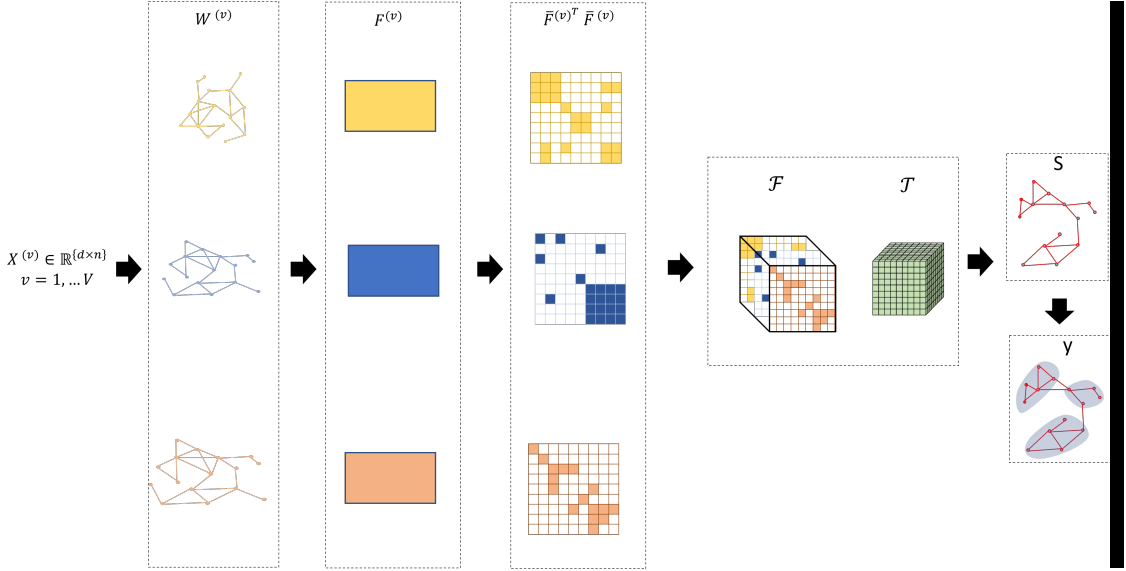


Figure 4.1: The proposed method framework

4.4. Solution. Since the problem consists of mainly 3 steps, each step can be solved separately.

The solution of the **first** step (3.1), which is called, an adaptive neighbor learning, is given in [27] and is a closed form solution:

$$s_{ij}^{(v)} = \left(-\frac{\|\mathbf{x}_i^{(v)} - \mathbf{x}_j^{(v)}\|_2^2}{2\gamma} + \eta_i \right)_+, \tag{4.2}$$

where η_i is the Lagrangian multiplier of the Lagrangian problem of (3.1) associated to the constraint $\mathbf{1}^T \mathbf{s}_i = 1$.

The paper made another assumption to learn sparse similarity matrix as it is shown that is robust to noise and outliers, it can be achieved by letting the point to only connect to their k-nearest neighbour, with this assumption, the value of regularization parameter γ is set to the

meaning of all γ_i [27]

$$\gamma = \frac{1}{2n} \sum_{i=1}^n \left(k \|\mathbf{x}_i^{(v)} - \mathbf{x}_{k+1}^{(v)}\|_2^2 - \sum_{j=1}^k \|\mathbf{x}_i^{(v)} - \mathbf{x}_j^{(v)}\|_2^2 \right) \quad (4.3)$$

and $\|\mathbf{x}_i^{(v)} - \mathbf{x}_j^{(v)}\|_2^2$ are ordered from small to larger with respect to j . η_i can be found [27] as

$$\eta_i = \frac{1}{k} + \frac{1}{2k\gamma_i} \sum_{j=1}^k \|\mathbf{x}_i^{(v)} - \mathbf{x}_j^{(v)}\|_2^2, \quad \gamma_i = \frac{k}{2} \|\mathbf{x}_i^{(v)} - \mathbf{x}_{k+1}^{(v)}\|_2^2 - \frac{1}{2} \sum_{j=1}^k \|\mathbf{x}_i^{(v)} - \mathbf{x}_j^{(v)}\|_2^2 \quad (4.4)$$

The **second** step (4.1), is an optimization problem over two variables, it is difficult to solve it directly, thus, we will use an alternate optimization algorithm. The problem can be transformed into two sub-problems, i.e., $F^{(v)}$ and \mathcal{T} sub-problems, and we alternately optimize each variable while the rest of the other variables are fixed, as follows:

$F^{(v)}$ -sub-problem: By fixing the other variable \mathcal{T} and since the matrices $\{F^{(v)}, v = 1 \dots, V\}$ are independent between them, we can decompose it to V independent problems, the equation (4.1) can be rewritten in matrix form as :

$$\begin{aligned} \min_{F^{(v)}} & \left[-\lambda \text{Tr} \left(F^{(v)\top} A^{(v)} F^{(v)} \right) + \frac{1}{2} \left\| \overline{F}^{(v)} \overline{F}^{(v)\top} - \mathcal{T}(:, v, :) \right\|_F^2 \right] \\ \text{s.t.} & F^{(v)\top} F^{(v)} = I_c. \end{aligned} \quad (4.5)$$

The equation (4.5) can be further rewritten as:

$$\begin{aligned} \min_{F^{(v)}} & \left[-\lambda \text{Tr} \left(F^{(v)\top} A^{(v)} F^{(v)} \right) + \frac{1}{2} \text{Tr} \left(\overline{F}^{(v)} \overline{F}^{(v)\top} \overline{F}^{(v)} \overline{F}^{(v)\top} \right) \right. \\ & \left. - \frac{1}{2} \text{Tr} \left(\overline{F}^{(v)} \overline{F}^{(v)\top} \left(\mathcal{T}(:, v, :) + \mathcal{T}(:, v, :)^T \right) \right) \right] \\ \text{s.t.} & F^{(v)\top} F^{(v)} = I_c. \end{aligned}$$

Let the diagonal matrix $P^{(v)} \in \mathbb{R}^{n \times n}$ be:

$$P^{(v)} = \text{diag} \left(\|f_i^{(v)}\|^{-1} \right), i = 1, \dots, n, \quad (4.6)$$

where the vector $f_i^{(v)}$ represents the i -th row of $F^{(v)}$. Hence, the normalized embedding matrix is given by:

$$\overline{F}^{(v)} = P^{(v)} F^{(v)}. \quad (4.7)$$

The optimization problem can be further rewritten as:

$$\begin{aligned} \max_{F^{(v)}} & \text{Tr} \left(F^{(v)\top} H^{(v)} F^{(v)} \right) \\ \text{s.t.} & F^{(v)\top} F^{(v)} = I_c, \end{aligned} \quad (4.8)$$

where $H^{(v)} = \lambda A^{(v)} + \frac{1}{2} P^{(v)} \left(\mathcal{T}(:, v, :) + \mathcal{T}(:, v, :)^T \right) P^{(v)} - \frac{1}{2} P^{(v)} \overline{F}^{(v)} \overline{F}^{(v)\top} P^{(v)}$.

Remark: The problem is now an optimization problem of trace on a manifold. The matrix

$H^{(v)}$ depends on the optimization problem $F^{(v)}$, which makes finding the optimal solution of $F^{(v)}$ thought to solve. Another difficulty, is that the function with respect to $F^{(v)}$ is not smooth (which is due the the inverse of the norm and hence, non differentiability on point zero), and thus not smooth. To manage to give an approximation, we use the Picard method, and since this is a sub-problem, we propose to consider $H^{(v)}$ as a function of the previous iteration, by this consideration, and since $H^{(v)}$ is symmetric, the solution would be well known, according to the Ky Fan's Theorem [28], are the eigenvectors normalized corresponding to the c largest eigenvalues of $H^{(v)}$.

For the k parameter of the adaptive neighbor, we can use the same value for all views, or use a different value for each view. We can also use a different value in the last step. The numerical result show that the same value if sufficient for all steps.

\mathcal{T} -sub-problem: By fixing the other variables, the equation (4.1) can be written as :

$$\min_{\mathcal{T}} \frac{1}{2} \|\mathcal{F} - \mathcal{T}\|_F^2 + \rho \|\mathcal{T}\|_{t-\gamma}. \quad (4.9)$$

The tensor \mathcal{T}^* that minimizes equation (4.9) is given in [7] as follows:

$$\mathcal{T}^* = \mathcal{U} * \Omega * \mathcal{V}^T, \quad (4.10)$$

where $\mathcal{F} = \mathcal{U} * \mathcal{S} * \mathcal{V}^T$ is the T-SVD of the tensor, and $\Omega \in \mathbb{R}^{n \times V \times n}$ is f-diagonal tensor. For $1 \leq i \leq \min(n, V) = V$ (since generally $V \leq n$), $1 \leq j \leq n$, the $\tilde{\Omega}_{i,i,j}$ is the limit point of Fixed Point Iteration:

$$\tilde{\Omega}(i, i, j)^{(k+1)} = \left(\tilde{\mathcal{S}}(i, i, j) - \frac{\rho\gamma(1+\gamma)}{\left(\gamma + \tilde{\Omega}(i, i, j)^{(k)}\right)^2} \right)_+, \quad (4.11)$$

where the fixed point converges to a local minimum after several iterations.

While the final solution is not the global optimal (NP-Hard), which is the case in most of this type of problems, the experiments show that the algorithm converges to a solution that produces promising results and even gives better results than the methods where the convergence is proven.

The last step: is similar to the first one, note that to avoid the need of further clustering algorithm on the obtained affinity matrix, we will make use of the next Theorem:

THEOREM 4.1. [29, 30] *The number of connected components in the non-negative similarity matrix of a graph is the same as the multiplicity of the eigenvalue 0 of its corresponding Laplacian matrix.*

Then, by adding a constraint of $\text{rank}(L_U) = n - c$ ensure that the obtained affinity matrix has exactly c connected components. However, the problem would be hard to tackle, thus the use of Ky Fan' Theorem; Since, $\sum_{i=1}^c \mathbf{v}_i(L_u) = 0$ is equivalent to $\text{rank}(L_U) = n - c$, where \mathbf{v}_i corresponds to the i -th smallest eigenvalue. Thus, we can write the problem as:

$$\min_{S, Q} \sum_{j=1}^n \left(\sum_{v=1}^V \left\| \mathbf{f}_i^{(v)} - \mathbf{f}_j^{(v)} \right\|_2^2 S_{ij}^{(v)} + \gamma s_{ij} \right) + \lambda \text{Tr}(Q^T L_S Q) \quad (4.12)$$

$$Q^T Q = I, Q \in \mathbb{R}^{n \times c}, \mathbf{1}^T \mathbf{s}_i = 1, s_{ij} \geq 0, i, j = 1, \dots, n,$$

Where λ is large enough, to make sure the last term $\text{Tr}(Q^T L_S Q) = 0$.

The problem can be solved using alternative optimization problem:

- When S is fixed, the problem becomes $\min \text{Tr}(Q^T L_S Q)$, $Q^T Q = I$, $Q \in \mathbb{R}^{n \times c}$, which is exactly Ky fan's Theorem.

- When Q is fixed, the problem is equivalent to:

$$\begin{aligned} \min_{s_i} & \|s_i + \frac{1}{2V\gamma} d_i\|_2^2 \\ \mathbf{1}^T \mathbf{s}_i &= 1, s_{ij} \geq 0, j = 1, \dots, n, \end{aligned} \quad (4.13)$$

with $d_{i,j} = \lambda \|\mathbf{q}_i - \mathbf{q}_j\|_2^2 + \sum_{v=1}^V \|\bar{\mathbf{f}}_i^{(v)} - \bar{\mathbf{f}}_j^{(v)}\|_2^2$, the solution with k-neighbour can be written in closed form as:

$$s_{ij} = \left(-\frac{d_{ij}}{2\gamma} + \eta_i \right)_+ , \quad (4.14)$$

where η_i, γ can be found similarly.

4.5. Algorithm. The following algorithm solves the last step in the problem:s

Algorithm 1 Solve (4.12)

Input: $\mathcal{F}^{(v)}$ (data), k (adaptive neighbor), c (cluster number).

Output: Affinity matrix S .

- 1: Initialize S by Adaptive neighbor without the rank constraint.
 - 2: **while** Not converged **do**
 - 3: Update Q ▷ Using Ky Fan's Theorem
 - 4: update S ▷ Using Eq. (4.14)
 - 5: **end while**
-

We can initialize $\lambda = \gamma$, then, at each iteration, increase it if the number of connected components found is smaller than c , and decrease it if greater than c . This is helpful in practice, and will accelerate the procedure.

The algorithm proposed to solve this problem is as follows:

Algorithm 2 Proposed method

Input: \mathcal{X} (data), k (adaptive neighbor), c (cluster number), γ (Norm parameter), λ (balance parameter). ρ (parameter)

Output: Consensus graph S , clustering result y

- 1: $H^{(v)} = 0$ ▷ Initialization
 - 2: Compute $S^{(v)}$. ▷ Via Eq. (4.2)
 - 3: Compute $A^{(v)}$. ▷ Using Eq. (3.3)
 - 4: **while** Not converged **do**
 - 5: Update $F^{(v)}$ ▷ Solution of Eq. (4.8)
 - 6: Update $P^{(v)}$ and $\bar{F}^{(v)}$ ▷ Using Eq. (4.6) and (4.7)
 - 7: Compute $\mathcal{F} = [\bar{F}^{(1)}\bar{F}^{(1)T}; \dots; \bar{F}^{(n)}\bar{F}^{(n)T}]$
 - 8: update \mathcal{T} ▷ Using Eq. (4.10)
 - 9: **end while**
 - 10: Compute S ▷ Via Algorithm 1
 - 11: Return the clustering result Y . ▷ Using k-means
-

The iteration (while loop) in the algorithm should stop when a condition criteria (convergence) is satisfied. The relative error in the objective function value will be used. We can also use the maximum number of iteration or running time.

The relative error can be calculated using the objective function of the previous and the current iteration

$$\frac{\text{Obj}(t) - \text{Obj}(t-1)}{\text{Obj}(t-1)} < \epsilon,$$

with ϵ is a threshold set generally as 1e-6.

5. Experiments. In this section, we do some experiments and compare our method with the state of art methods.

5.1. Data sets. We used multiple different real world data sets, that are commonly used in the literature. The majority of image multi-view data sets are derived from initial single-view image data sets.

- *One-hundred plant species leaves data set leafs (100Leaves)*¹: It consists of 1600 samples, of 100 different species, 4 views are given: shape descriptor, fine scale margin and texture histogram.
- *3 sources data set (3Sources)*²: It consists of 169 news, provided by three news companies, including the BBC, Reuters, and The Guardian. Each piece of news was manually labeled with one of six relevant designations.
- *Handwritten digit data set(HW)*³: It is from the UCI repository. It consists of 2000 samples of handwritten digits, with a 6 views, It has 10 clusters (0-9).

The characteristics of these raw feature data sets are given in the table 5.1 below, which displays the number of samples n , the number of views V , the cluster number c , and the dimension of features in view d_v . More details can be found regarding the dataset using the hyperlinks in the footnotes.

¹[https://archive.ics.uci.edu/ml/data sets/One-hundred+plant+species+leaves+data+set](https://archive.ics.uci.edu/ml/data%20sets/One-hundred+plant+species+leaves+data+set)

²[http://elki.dbs.ifi.lmu.de/wiki/data sets/MultiView](http://elki.dbs.ifi.lmu.de/wiki/data%20sets/MultiView)

³<http://archive.ics.uci.edu/ml/datasets/Multiple+Features>

Table 5.1: Summary of the benchmark data sets used

Data set	# samples	# views	# clusters	d_1	d_2	d_3	d_4	d_5	d_6
3Sources	169	3	6	3560	3631	3068	-	-	-
100Leaves	1600	3	100	64	64	64	-	-	-
HW	2000	6	10	216	76	64	6	240	47

5.2. Compared methods. In order to work with the same data set and the same clustering metrics, a few modifications were made to these data sets prior to evaluating the state-of-the-art methods.

- **MVGL**⁴ This method optimizes the joint graph with a rank constraint and treats data as matrices without any tensor related used.
- **CGL**⁵ This method integrates adaptive neighbour and finds the fusion graph in a new subspace using the a convex norm.
- **MV-LRSCC**⁶ This method jointly learns a low-rank representation and sparse subspace clustering across multiple views. It has 4 variants, i.e., pairwise, centroid, pairwise kernel, and centroid kernel.
- **AMGL**⁷ This method learns the wights of each graph automatically and without the need of any parameter.

5.3. Evaluation metrics. To randomize the tests, each algorithm is executed ten times. Using well-known benchmark data sets, several metrics are used to assess how effectively these multi view clustering methods perform. Multiple measurements favor different features in the clustering task, which motivates us to employ more than one. The accuracy (ACC), the normalized mutual information (NMI), the F1 measure (F-measure), and the adjusted rand index (ARI) are the main ones used; see [9] for more details on these measures A higher number for each measure reflects better clustering performance.

5.4. Computation complexity. We can calculate the computation complexity of our method. The first step of computing the similarity matrices needs $\mathcal{O}(n \log(n)V)$, normalizing it needs $\mathcal{O}(n^2V)$, computing $H^{(v)}$ needs $\mathcal{O}(n^2)$, computing the c largest eigenvectors of $F^{(v)}$ is $\mathcal{O}(n^2c)$, and computing \mathcal{T} needs $\mathcal{O}(n^2V \log(n) + n^2V^2 + nVw)$, where w is the maximum number of iterating of the fixed point(usually not very large), the first part represent the FFT and IFFT costs, and the second, represents the SVD cost. Computing S takes the same amount as the first step, it needs $\mathcal{O}(n \log(n))$. Finally, the spectral clustering needs $\mathcal{O}(n^2c)$. In total, the complexity of the proposed model is $\mathcal{O}\left(n^2(c + V) + n \log(n) + tn^2V\left(c + \log(n) + V + \frac{w}{n}\right)\right)$, where t is the number of iteration.

We also compare the time cost of each method on each dataset.

⁴<https://github.com/kunzhan/MVGL>

⁵<https://github.com/guanyuezhen/CGL>

⁶<https://github.com/mrbic/Multi-view-LRSCC>

⁷<https://github.com/kylejingli/AMGL-IJCAI16>

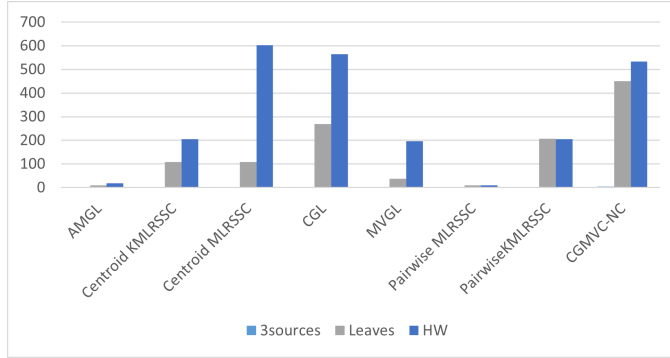


Figure 5.1: Time cost of different methods per second.

Which shows that our method, even it has a non-convex part, it takes generally as much time as most of the benchmark methods. The dataset 3Sources is quite small compared to the others, which is why it is quite has low time cost.

5.5. Parameter setting. The parameters value of each methods were chosen as suggested from their papers, along with other values that are near the suggested ones and we report the best value by accuracy since we have multiple evaluation metrics.

In our suggested model, the parameters are γ is chosen from the range $[10^{-4}, 10^{-3}, 10^{-2}, 10^{-1}, 1, 10, 10^2]$, we found that setting γ to 0.1 works best in all cases. For λ , we follow the suggested in the CGL paper and we set it to $\frac{1}{\sqrt{\min(N_1, N_3)}}$. For the parameter ρ , we've tried in the $[10^{-4}, 10^{-3}, 10^{-2}, 10^{-1}, 1, 10, 10^2]$, the experiments suggests that the value has not a decisive effect.

For some methods, a post clustering (e.g., k-means) is needed on the obtaining embedding data, as it is sensitive to initial values, we repeat the k-means clustering processing 20 trials to avoid the randomness perturbation and report the result with the lowest value for the objective function of k-means clustering among the 20 results. The maximum number of iteration in all methods is set to 100.

5.6. Comparison result and analysis. The comparison results are shown in tables 5.4, 5.3, and 5.2. The best and second best value of each measure is shown in bold and underlined, respectively. We note that the standard deviation is avoided to be show for the k-means clustering trials since simply, not all the methods employ it, we mention that the values are rounded to the ten-thousandths.

Table 5.2: Clustering measure on HW data set

Method	Fscore	Precision	Recall	NMI	ARI	ACC	Purity
AMGL	0,4011	0,3081	0,5788	0,6162	0,3115	0,5536	0,5893
MVGL	0.6367	0.5570	0.7429	0.7231	0.5900	0.6895	0.7245
Pairwise MLRSSC	0,7264	<u>0,8627</u>	0,6276	0,7998	0,6907	0,747	<u>0,9185</u>
Pairwise KMLRSSC	0,5399	0,6179	0,4794	0,5958	0,4818	0,6361	0,7412
Centroid KMLRSSC	0,5399	0,6179	0,4794	0,5958	0,4818	0,6361	0,7412
Centroid MLRSSC	0,7266	0,8678	0,6250	0,8021	0,6907	0,7438	0,9244
CGL	0,8584	0,7941	0,9630	0,9354	0,8405	0,8617	0,8741
CGMVC-NC	0.8996	0.8395	0.9853	0.9498	0.8874	0.8929	0.8996

Table 5.3: Clustering measure on 3sources data set

Method	Fscore	Precision	Recall	NMI	ARI	ACC	Purity
AMGL	0.2765	0.1711	0.7604	0.8490	0.2652	0.6352	0.7028
MVGL	0.3455	0.2255	0.7381	0.1522	0.0163	0.3846	0.4320
Pairwise MLRSSC	<u>0.6443</u>	0.6045	0.6969	0.6167	<u>0.5460</u>	<u>0.6840</u>	0.7491
Pairwise KMLRSSC	0.4675	0.3798	0.6118	0.4837	0.3525	0.5098	0.5240
Centroid MLRSSC	0.5662	0.4629	<u>0.7492</u>	0.6470	0.4725	0.6482	0.6683
Centroid KMLRSSC	0.4745	0.3847	0.6214	0.4824	0.3620	0.5169	0.5272
CGL	0.6224	<u>0.7097</u>	0.5555	<u>0.6800</u>	0.5263	0.6604	<u>0.7976</u>
CGMVC-NC	0.6670	0.7218	0.6213	0.6747	0.5760	0.7047	0.8133

Table 5.4: Clustering measure on 100Leaves data set

Method	Fscore	Precision	Recall	NMI	ARI	ACC	Purity
AMGL	0,2765	0,1711	<u>0,7604</u>	<u>0,8490</u>	0,2652	0,6352	0,7028
MVGL	0.3455	0.2255	0.7381	0.1522	0.0163	0.3846	0.4320
Pairwise MLRSSC	0,0102	0,6703	0,0245	0,3434	0,0297	0,0633	0,7702
Pairwise KMLRSSC	0,1120	0,8365	0,0600	0,5401	0,0962	0,0800	0,8911
Centroid MLRSSC	0,0492	0,6232	0,0256	0,3583	0,0317	0,0732	0,7374
Centroid KMLRSSC	0,0517	0,6128	0,0270	0,3634	0,0343	0,0736	0,7306
CGL	0,6245	0,7097	0,5654	0,6871	<u>0,5263</u>	0,6604	0,8024
CGMVC-NC	<u>0.7521</u>	<u>0.6407</u>	0.9235	0.9476	0.7493	0.7936	<u>0.8142</u>

Our proposed approach performs well on the benchmark datasets. It outperforms the other methods on the accuracy evaluation metric, and does generally well, on the rest of the evaluation metrics. It performs better than the CGL on almost all the metrics over the different dataset.

6. Conclusion. In conclusion, the proposed method for multi-view clustering using a non-convex tensor norm has shown promising results in improving the clustering accuracy compared to traditional methods. By incorporating the tensor structure of multi-view data, the proposed method can effectively capture the underlying correlations between different views, leading to more accurate clustering results. Despite the non-convexity of the tensor norm, the

proposed method can still be optimized efficiently using existing algorithms. Overall, CGMVC-NC provides a valuable tool for multi-view data analysis and has the potential to enhance our understanding of complex systems in various fields, including computer vision, neuroscience, and social network analysis. Further research can explore the application of this method to other types of data and the extension to other machine learning tasks.

REFERENCES

- [1] Tamara G Kolda and Brett W Bader. Tensor decompositions and applications *. *Society for Industrial and Applied Mathematics*, 51:455–500, 2009.
- [2] Evrim Acar and Bülent Yener. Unsupervised multiway data analysis: A literature survey. *IEEE Transactions on Knowledge and Data Engineering*, 21:6–20, 1 2009.
- [3] Misha E. Kilmer and Carla D. Martin. Factorization strategies for third-order tensors. *Linear Algebra and its Applications*, 435:641–658, 8 2011.
- [4] Misha E Kilmer, Karen Braman, Ning Hao, and Randy C Hoover. Third-order tensors as operators on matrices: A theoretical and computational framework with applications in imaging. *SIAM Journal on Matrix Analysis and Applications*, 34(1):148–172, 2013.
- [5] Ning Hao, Misha E Kilmer, Karen Braman, and Randy C Hoover. Facial recognition using tensor-tensor decompositions. *SIAM Journal on Imaging Sciences*, 6(1):437–463, 2013.
- [6] Canyi Lu, Jiashi Feng, Yudong Chen, Wei Liu, Zhouchen Lin, and Shuicheng Yan. Tensor robust principal component analysis with a new tensor nuclear norm. *IEEE Transactions on Pattern Analysis and Machine Intelligence*, 2020.
- [7] Shuting Cai, Qilun Luo, Ming Yang, Wen Li, and Mingqing Xiao. Tensor robust principal component analysis via non-convex low rank approximation. *Applied Sciences 2019, Vol. 9, Page 1411*, 9:1411, 4 2019.
- [8] Zhao Kang, Chong Peng, Qiang Cheng, and Qiang Cheng. Robust pca via nonconvex rank approximation. *arXiv: Computer Vision and Pattern Recognition*, 2015.
- [9] Alaeddine Zahir, Khalide Jbilou, and Ahmed Ratnani. Multilinear algebra methods for higher-dimensional graphs. *Applied Numerical Mathematics*, 2023.
- [10] Guangcan Liu, Zhouchen Lin, and Yong Yu. Robust subspace segmentation by low-rank representation. In *Proceedings of the 27th International Conference on International Conference on Machine Learning*, ICML’10, page 663–670, Madison, WI, USA, 2010. Omnipress.
- [11] Ehsan Elhamifar and René Vidal. Sparse subspace clustering: Algorithm, theory, and applications. *IEEE Transactions on Pattern Analysis and Machine Intelligence*, 35(11):2765–2781, 2013.
- [12] Shirui Luo, Changqing Zhang, Wei Zhang, and Xiaochun Cao. Consistent and specific multi-view subspace clustering. *Proceedings of the AAAI Conference on Artificial Intelligence*, 32, 4 2018.
- [13] Xiaochun Cao, Changqing Zhang, Huazhu Fu, Si Liu, and Hua Zhang. Diversity-induced multi-view subspace clustering. In *2015 IEEE Conference on Computer Vision and Pattern Recognition (CVPR)*, pages 586–594, 2015.
- [14] Yu Xiang Wang, Huan Xu, and Chenlei Leng. Provable subspace clustering: When lrr meets ssc. *Advances in Neural Information Processing Systems*, 2013.
- [15] Jianlong Wu, Zhouchen Lin, and Hongbin Zha. Essential tensor learning for multi-view spectral clustering. *IEEE Transactions on Image Processing*, 28(12):5910–5922, 2019.
- [16] Deyan Xie, Quanxue Gao, Siyang Deng, Xiaojun Yang, and Xinbo Gao. Multiple graphs learning with a new weighted tensor nuclear norm. *Neural Networks*, 133:57–68, 2021.
- [17] Miaomiao Cheng, Liping Jing, and Michael K. Ng. Tensor-based low-dimensional representation learning for multi-view clustering. *IEEE Transactions on Image Processing*, 28:2399–2414, 5 2019.
- [18] Kamalika Chaudhuri, Sham M Kakade, Karen Livescu, and Karthik Sridharan. Multi-view clustering via canonical correlation analysis. In *Proceedings of the 26th annual international conference on machine learning*, pages 129–136, 2009.
- [19] Tian Xia, Dacheng Tao, Tao Mei, and Yongdong Zhang. Multiview spectral embedding. *IEEE Transactions on Systems, Man, and Cybernetics, Part B: Cybernetics*, 40:1438–1446, 12 2010.
- [20] Feiping Nie, Jing Li, and Xuelong Li. Parameter-free auto-weighted multiple graph learning: A framework for multiview clustering and semi-supervised classification. In *Proceedings of the Twenty-Fifth International Joint Conference on Artificial Intelligence, IJCAI’16*, page 1881–1887. AAAI Press, 2016.
- [21] Feiping Nie, Guohao Cai, and Xuelong Li. Multi-view clustering and semi-supervised classification with

- adaptive neighbours. *AAAI*, 2017.
- [22] Feiping Nie, Jing Li, and Xuelong Li. Self-weighted multiview clustering with multiple graphs. In *Proceedings of the Twenty-Sixth International Joint Conference on Artificial Intelligence, IJCAI-17*, pages 2564–2570, 2017.
- [23] Yongyong Chen, Xiaolin Xiao, and Yicong Zhou. Multi-view clustering via simultaneously learning graph regularized low-rank tensor representation and affinity matrix. *2019 IEEE International Conference on Multimedia and Expo (ICME)*, pages 1348–1353, 2019.
- [24] Haiyan Wang, Guoqiang Han, Junyu Li, Bin Zhang, Jiazhou Chen, Yu Hu, Chu Han, and Hongmin Cai. Learning task-driving affinity matrix for accurate multi-view clustering through tensor subspace learning. *Information Sciences*, 563:290–308, 7 2021.
- [25] Yujiao Zhao, Yu Yun, Xiangdong Zhang, Qin Li, and Quanxue Gao. Multi-view spectral clustering with adaptive graph learning and tensor Schatten p -norm. *Neurocomputing*, 468:257–264, 1 2022.
- [26] Zhenglai Li, Chang Tang, Xinwang Liu, Xiao Zheng, Wei Zhang, and En Zhu. Consensus graph learning for multi-view clustering. *IEEE Transactions on Multimedia*, 24:2461–2472, 2022.
- [27] Feiping Nie, Xiaoqian Wang, and Heng Huang. Clustering and projected clustering with adaptive neighbors. *Knowledge Discovery and Data Mining*, 2014.
- [28] Mathematics: K Y Fan, H J Muller, J Genet, C W Metz, M L Bozeman, Carnegie Inst, J P Reynolds, B B Harris, and K W Cooper. On a theorem of weyl concerning eigenvalues of linear transformations i. *Proceedings of the National Academy of Sciences*, 35:652–655, 11 1949.
- [29] Bojan Mohar, Y Alavi, G Chartrand, and OR Oellermann. The laplacian spectrum of graphs. *Graph theory, combinatorics, and applications*, 2(871-898):12, 1991.
- [30] Fan RK Chung. *Spectral graph theory*, volume 92. American Mathematical Soc., 1997.